Miniaturized Magnetostrictive Antennas for Wireless Sensing Applications

by

Baju Chiyezhath Joy

B.Tech Indian Institute of Technology Madras (2019)

Submitted to the Department of Mechanical Engineering in partial fulfillment of the requirements of the degree of Master of Science at the

MASSACHUSETTS INSTITUTE OF TECHNOLOGY

September 2021

Signature of Author: ……………………………………………………………………...

Baju Chiyezhath Joy
Department of Mechanical Engineering
August 13, 2021

Certified by: …………………………………………………………………………

Prof. Deblina Sarkar
Assistant Professor of Media Arts and Sciences
Thesis Supervisor

Certified by: …………………………………………………………………………

Prof. Jeehwan Kim
Associate Professor of Mechanical Engineering and Material Science and Engineering
Thesis Reader

Accepted by: ……………………………………………………………………….

Prof. Nicolas Hadjiconstantinou
Chairman, Department Committee on Graduate Theses

Abstract

Magnetostrictive (MES) antennas have been widely used for wireless sensing applications. Miniaturization of MES antennas can open new applications in in-vivo wireless sensing with higher spatial resolution and solve challenges involved in the miniaturization of conventional electromagnetic antennas. In this thesis two different methods have been explored for easy and fast fabrication of miniaturized MES antennas down to sub-mm sizes from the amorphous magnetostricive film Metglas 2826 MB and their advantages and disadvantages have been studied. Laser micromachining is shown to be a more versatile method compared to fabrication using Diesaw to fabricate antennas of different shapes easily. The frequency response of the fabricated antennas is first studied in air and characterized using Finite Element Analysis and analytical modelling to characterize the quality factor and magnetomechanical coupling efficiency. The antennas are then tested in water to understand the effects of viscous damping on antenna response and check the feasibility of sensing in liquid or wet environment. After characterization, a highly sensitive pH sensitive MES antenna of size 6 mm x 1 mm x 28 um with a sensitivity of 15 kHz/pH is fabricated using a pH sensitive copolymer of Acrylic Acid and Isooctyl Acrylate and characterized using solutions of different pH. The challenges involved in further miniaturization of the sensors and future work is also discussed.

Acknowledgements

I would like to thank my supervisor Prof. Deblina Sarkar for giving me the opportunity to learn a variety of exciting topics and skills, instilling in me the passion for research and entrusting me with a challenging and impactful project during my Masters degree. You have been an amazing advisor in guiding me as I made my first steps into graduate studies. I would also like to thank David Bono for all his help in the last two years for building the setups for my project and teaching me all your tips and tricks in doing experiments. You have been the most resourceful person I met in MIT, and the fact that you help a large number of students with their projects is truly amazing and inspirational. I would also like to thank my Meche advisor Prof. Jeehwan Kim for introducing me to world of microfabrication and 2d materials through your courses. The last two years would not have been enjoyable without my amazing labmates: my partner in crime- aaShubham aka PDMS, Yubin, Shivam, Benoit and Marta. Special thanks to all of you for all the wonderful moments together, for your selfless help and for keeping me sane the last two years. Also special thanks to my friend Joshua who insisted he be thanked in the acknowledgement. None of this would be possible without my most supportive and awesome family Appa, Amma and Roshan. Finally, you guys get to see me graduate in style!!

Table of Contents

List of Figures

List of Tables

Chapter 1

Introduction

Sensors are critical in a wide variety of fields such as manufacturing, transportation, health monitoring, aerospace engineering, weather monitoring etc. Wireless sensing which involves sensing of an analyte such as a chemical, gas or biomolecule remotely using light, radio frequency (RF) electromagnetic waves, or acoustic waves is especially important for biological applications because it can enable non-invasive or minimally invasive sensing of various analytes for health monitoring and therapeutics. In recent years there has been an interest in the use of magnetoelastic or magnetostrictive antennas for wireless sensing applications due to their ability to wirelessly sense a wide variety of analytes, ease of miniaturization and operation using low frequency electromagnetic waves [1]. Small sizes help in sensing various analytes with higher spatial resolution thereby creating a wider range of applications. Low frequency of operation becomes critical for in-vivo applications due to attenuation of high frequency electromagnetic waves in biological tissues. In this thesis the miniaturization and possible wireless sensing applications using magnetoelastic sensors is explored.

1.1 Magnetostriction

Magnetostrictive antennas work on the principle of magnetostriction which is the phenomenon by which a material gets strained in response to magnetization and vice versa. Magnetostriction can be visualized as shown in Fig. 1.1 in which magnetization of the material by an applied magnetic field causes the magnetic domains to align in one direction causing a strain in the material. Magnetostricion (λ) is defined as the strain in the material in response to a magnetic field and has a nonlinear relation with magnetic field strength as shown in Fig. 1.2. Hence when a thin film made of a magnetostricitve material is excited using a small AC magnetic field a mechanical resonance is observed when the frequency of excitation of AC magnetic field matches the natural frequency of vibration of the thin film. This phenomenon is used to design magnetostrictive (MES) antennas which are passive devices similar to RFIDs which can be interrogated remotely using a magnetic field and detected wirelessly by inductive coupling using a coil. To maximize the strain in response to the small signal perturbation the material is biased using a DC magnetic field as shown in Fig 1.2 thereby maximizing the magnetostritctivity ($\boldsymbol{d} = \frac{\boldsymbol{d\lambda}}{\boldsymbol{dH}}$). MES antennas are promising alternatives to conventional electromagnetic antennas due to their ease of miniaturization and low frequency of operation as discussed below.

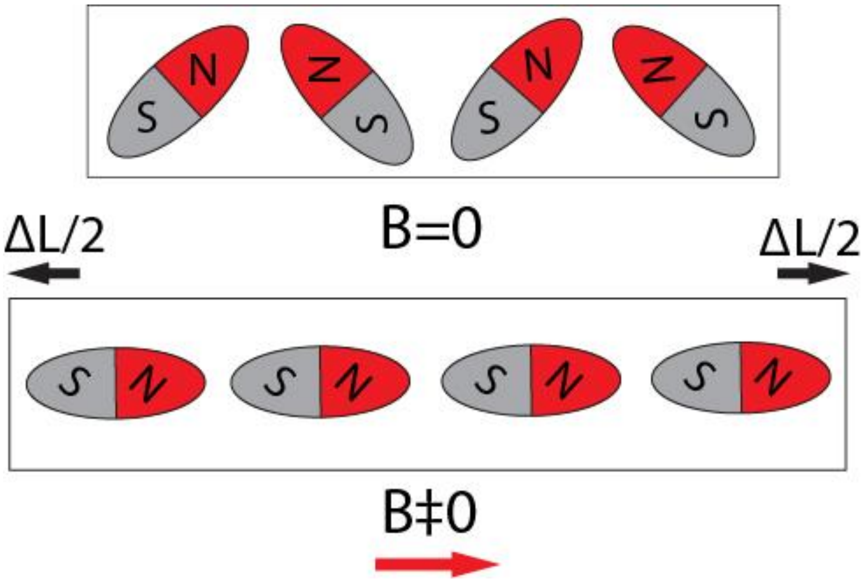

Figure 1. 1 Schematic representation of the principle of magnetostriction. The red and grey sections denote the north and south poles of the magnetic domains respectively. A non-zero magnetic flux density (B) produces a strain (ΔL) in the material.

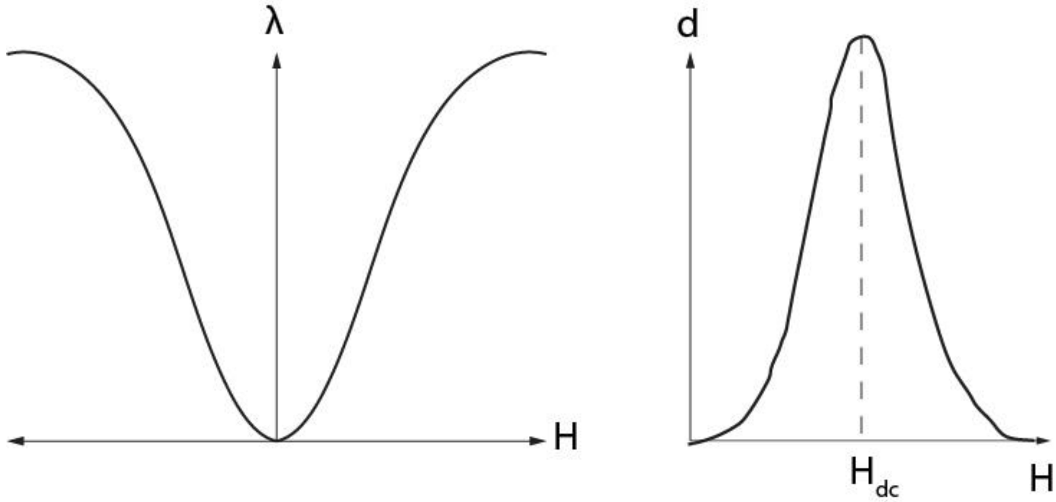

Figure 1. 2 Schematic representation of the dependence of magnetostriction and magnetostrictivity on magnetic field strength (H). Optimum DC bias (H_{dc}) is also shown.

1.2 Advantages of MES Antennas

Electromagnetic antennas which operate on the principle of electromagnetic resonance have sizes close to the wavelength of the radiated EM wave and hence have large sizes when operating in MHz or low GHz frequencies (several centimeters to meters) [2]. Since MES antennas operate on the principle of acoustic resonance MES antennas of similar sizes operate at much lower frequencies compared to an EM antenna of the same size. Low frequency of operation (< 1GHz) is critical for in-vivo wireless sensing applications due to signal loss and heating effects in biological tissues at higher frequencies ([3], [4]). For example, a sub-mm MES antenna of size 500 um operates at a frequency of approximately 4.5 MHz compared to an EM antenna of similar size which operates at a frequency of approximately 100s of GHz. Hence miniaturization of conventional EM antennas for biological applications has been a challenge ([5], [6]) and MES antennas are considered a promising alternative [7].

1.3 Sensing Using MES Antennas

Since MES antennas are passive devices, to enable sensing of various analytes the antennas are chemically functionalized to produce a mass change in response to change in the concentration of the analyte of interest, thereby changing the resonance frequency of the antenna as illustrated in Fig 1.3. The concentration of the analyte can be calibrated to the resonance frequency using in vitro experiments and can later be used for in-vivo sensing applications. It will be shown that the sensitivity of the antenna increases as the size of the antenna decreases, meaning miniaturization would help in improving the sensitivity along with the obvious advantage of sensing a quantity with better spatial resolution. Magnetoelastic sensors have been previously shown to sense force, viscosity, bacterial concentration, humidity, carbon dioxide, ammonia, and pH [1]. The fabrication of the sensors is mainly done by dicing an amorphous magnetostrictive film using a Diesaw followed by annealing at high temperature to remove residual stresses [8].

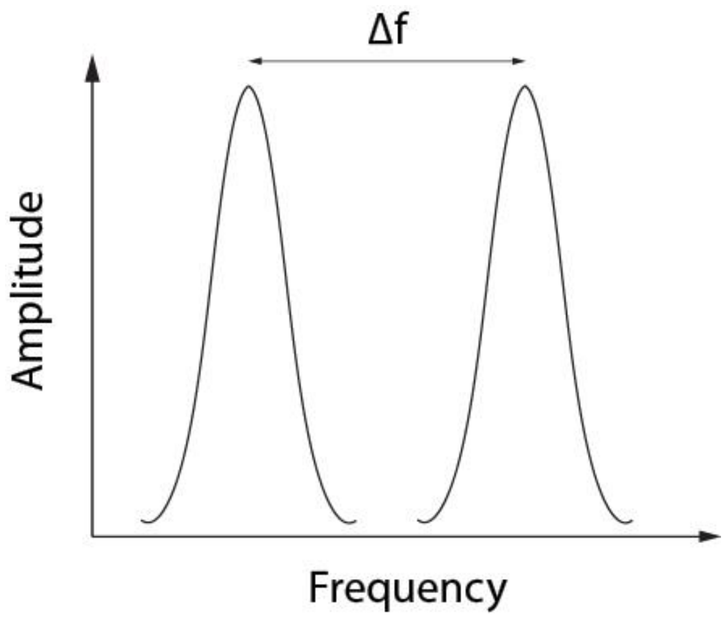

Figure 1. 3 Schematic representation of resonance frequency shift (Δf) produced due to mass loading.

1.4 Thesis Outline

The objective of this thesis is to explore different methods for the fabrication of miniaturized MES antennas (few millimeters to sub-mm sizes), characterize the frequency response of the fabricated antennas in air and water and fabricate a highly sensitive antenna for pH sensing. Chapter 2 discusses the fabrication of MES antennas using Diesaw and Laser Micromachining. The advantages and disadvantages of the two methods are also discussed. Chapter 3 describes the characterization of the MES antennas in air and water. The antenna response is modelled using Finite Element Analysis and analytical modelling to characterize the magnetomechanical coupling coefficient and quality factor of the fabricated antennas. Chapter 4 discusses the synthesis of a pH responsive mass changing polymer and functionalization of a 6 mm MES antenna with the polymer to fabricate a highly sensitive pH sensor which can work in liquid media. Chapter 5 concludes the thesis and discusses the future work.

Chapter 2

Fabrication of MES Antennas

2.1. Introductory Remarks

Two different methods have been explored to fabricate miniaturized MES antennas from a 28 um thick Metglas 2826 MB magnetostrictive film. The first method involves dicing of the film using a DAD-3240 diesaw and has been previously reported for fabrication magnetoelastic resonators [8]. The second method explored is more versatile and involves laser micromachining of the film using an Oxofrd 532 nm laser. The two methods are discussed in detail in this section along with their advantages and disadvantages.

2.2. Diesaw

Fig. 2.1 shows the schematic diagram which illustrates the fabrication of MES antennas using a DAD-3240 Diesaw. The magnetostrticitve film is first fixed to a Silicon wafer using two layers of temperature curable epoxy and Kapton tape. This prevents the diced resonators from being washed away by the water jet used for cooling the Diesaw blade. A 30 um thick diamond blade is used for machining the film at a feed speed of 3 mm/s.

Rectangular shaped MES antennas of required sizes are diced by traversing the blade in a grid-like format. After dicing the wafer is ultrasonicated in Acetone for 30 min, multiple times to remove the epoxy and release the antennas into solution. The antennas are then collected using a permanent magnet. They are then annealed for 2 hours at 220 °C, in a vacuum oven at 50 mTorr pressure to release any residual stresses. Resonators of sizes ranging from 6 mm x 1 mm x 28 um to 500 um x 200 um 28 um were fabricated using this method. Fig. 2.2 shows an optical image of 500 um x 300 um x 28 um resonator fabricated using the Diesaw.

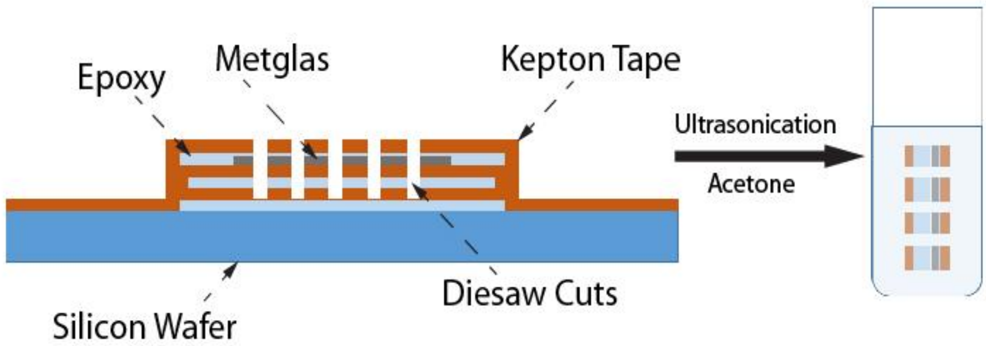

Figure 2. 1 Schematic representation of fabrication of MES antennas using a Diesaw

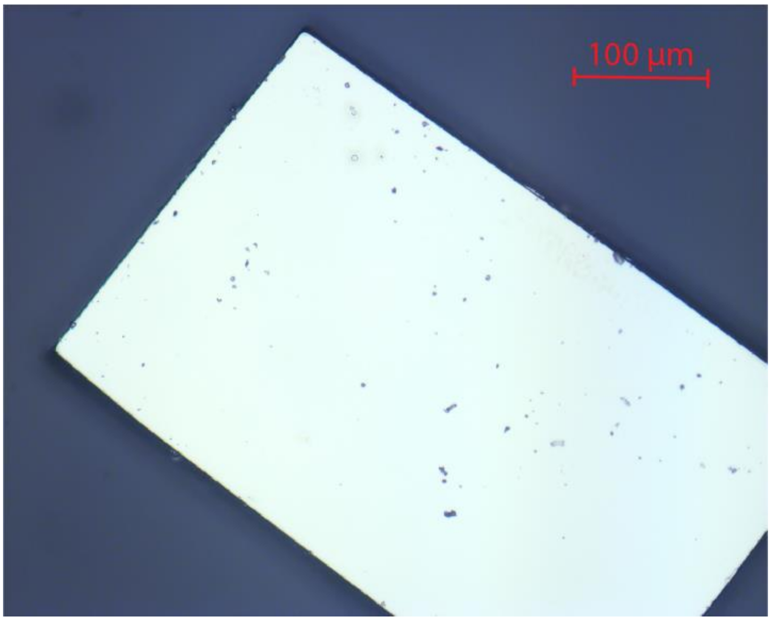

Figure 2. 2 Optical Image showing a 500 um x 300 um x 28 um MES Antenna fabricated using Diesaw

2.3. Laser Micromachining

Fig. 2.3 shows the schematic diagram which illustrates the fabrication of MES antennas using an Oxford 532 nm laser of 5 W power. The Metglas film is fixed on a Silicon wafer using a large permanent magnet fixture below the wafer. The Silicon wafer helps in dissipating the heat generated during machining since it has a high thermal conductivity. Replacing the Silicon wafer with a glass slide was found to produce resonators which were brittle and had very poor frequency responses, since the film gets heated up due to the poor conductivity of glass. The permanent magnet helps in making good thermal contact between the Silicon wafer and the film and prevents bowing of the film during machining. The permanent magnet is fixed on an XY stage which can be programmed to fabricate resonators of any shape and size. The feed, pulse frequency, laser power and number of passes were optimized to ensure minimum heating and good resonator response during experiment. A pulse frequency of 20 kHz, feed speed of 1 mm/s, 1% laser power and 50 passes were found to be ideal for fabricating resonators of sizes of the order of 500 um x 200 um x 28 um. The fabricated resonators can be easily collected using a permanent magnet. Post processing annealing of the fabricated antennas was not found to improve the resonator response. Resonators of sizes ranging from 6 mm x 1 mm x 28 um to 400 um x 200 um x 28 um were fabricated using this method. Fig 2.4 shows an optical image of 500 um x 200 um x 28 um resonator with round edges fabricated using laser micromachining.

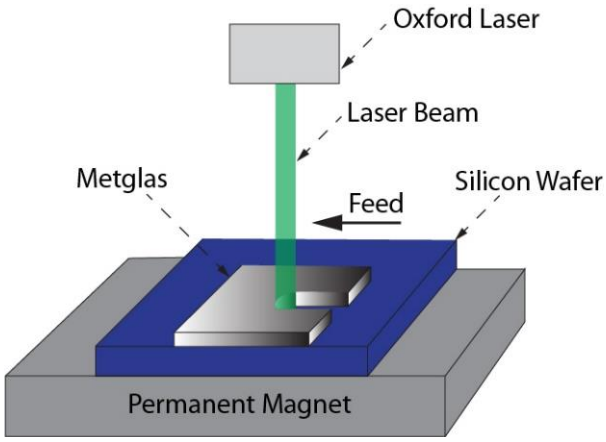

Figure 2. 3 Schematic diagram showing the setup for fabrication of MES antennas using laser micromachining

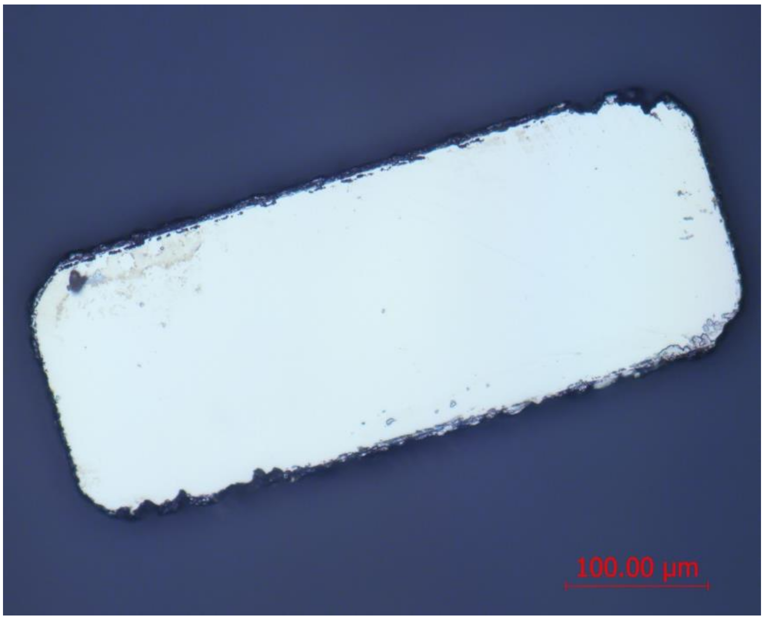

Figure 2. 4 Optical Image showing a 500 um x 200 um x 28 um MES Antenna fabricated using Laser Micromachining

2.4. Discussion

Fabrication using Diesaw is most suitable for fabricating a large number of rectangular shaped resonators in the shortest time. Also, it can be seen from Fig 2.2 that it gives very flat resonator sidewalls. It suffers from the disadvantage that it is not ideal for fabricating a resonator of custom design or a resonator having round edges. Also, this method requires lengthy sample preparation and post processing steps. Both of these disadvantages are overcome by using laser micromachining. Laser micromachining can be used for fabricating any resonator shape by programming the XY motion of the stage. Also sample preparation for fabrication is relatively simple and no post processing annealing is required. The sidewalls of the fabricated antennas were not perfectly flat but the responses of antennas fabricated by both methods were found to be almost identical. Laser micromachining is also more suitable for further miniaturization of the antennas since it can create features as small as 20 um easily [9]. Resonators with features smaller than 200 um produced chipped edges on the Diesaw and had poor frequency responses. Future work involves optimization of laser parameters to obtain more flat sidewalls and smaller resonators. The smallest resonator fabricated using laser micromachining which is of dimensions 400 um x 200 um x 28 um is shown in Fig. 2.5.

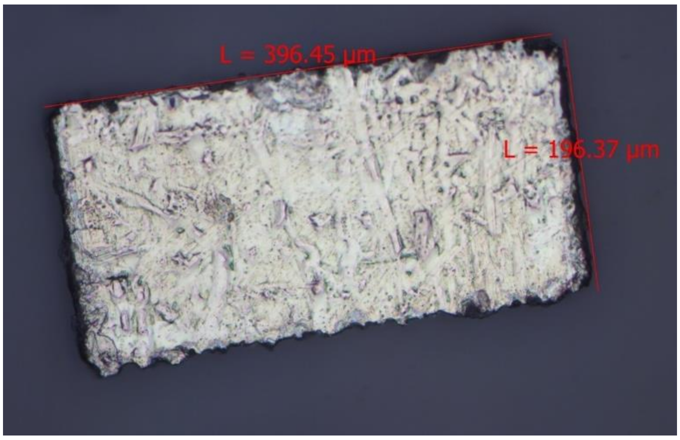

Figure 2. 5 Optical Image showing a 400 um x 200 um x 28 um MES Antenna fabricated using Laser Micromachining

Chapter 3

Characterization and Modelling of MES Antennas

3.1 Introductory Remarks

This section discusses the preliminary experiments performed for characterizing and modelling the frequency response of MES antennas in air and water. Two different methods have been used for wireless detection of MES antennas by inductive coupling using a coil. The first method involves measuring the voltage across the coil containing the antenna using a Lock-in Amplifier and the second method involves measuring the S-parameters of the coil containing the resonator using a Vector Network Analyzer (VNA). Both methods are discussed in detail in this section. The fabricated MES antennas were first measured in air and the resonator response was then modelled using Finite Element Analysis and analytical equations to understand the frequency response and calculate the values of useful material properties. The antennas were then measured in water and the quality factor and resonance frequency change due to viscous damping and mass loading effects was studied to understand how well the resonators can function in a wet environment which will be crucial for in-vivo sensing applications.

3.2 Measurement Methods

3.2.1 Vector Network Analyzer (VNA)

Fig 3.1 shows a schematic diagram which illustrates the wireless detection of MES antennas using a VNA. The setup consists of a Receiving (Rx) coil wound around a capillary tube. The antenna is inserted into the coil during measurement and a permanent magnet is used for applying the required optimum DC bias. The resonator length is oriented along the axis of the coil such that the excitation AC magnetic field is along the length of the resonator. The coil is connected to Port-1 of the VNA and the S11 or reflection coefficient of the coil is measured as a function of frequency. At the mechanical resonance frequency, a dip in the S11 is observed which is due to the increase in effective permeability of the resonator at resonance which causes a change in the impedance of the coil. Fig 3.2 a, b and c shows the detected response in air for antennas having dimensions of 6 mm x 1 mm x 28 um, 5 mm x 1 mm x 28 um and 1 mm x 500 um x 28 um respectively. The resonance frequency increases as the size of the antenna decreases, and is roughly given by the natural frequency of vibration of a thin film resonator of length L excited in the longitudinal mode:

$$\boldsymbol{f_r} = \frac{\mathbf{1}}{\mathbf{2}\boldsymbol{L}}\sqrt{\frac{\boldsymbol{E}}{\boldsymbol{\rho}(\mathbf{1}-\boldsymbol{\nu})}} \tag{3.1}$$

where E is the Young's modulus, ρ is the density and ν is the Poisson's ratio of the material. The Lock-in Amplifier setup discussed below using a gradiometer coil is more sensitive for detecting small changes in magnetization and hence is more ideal for the detection of antennas smaller than 1 mm x 500 um x 28um.

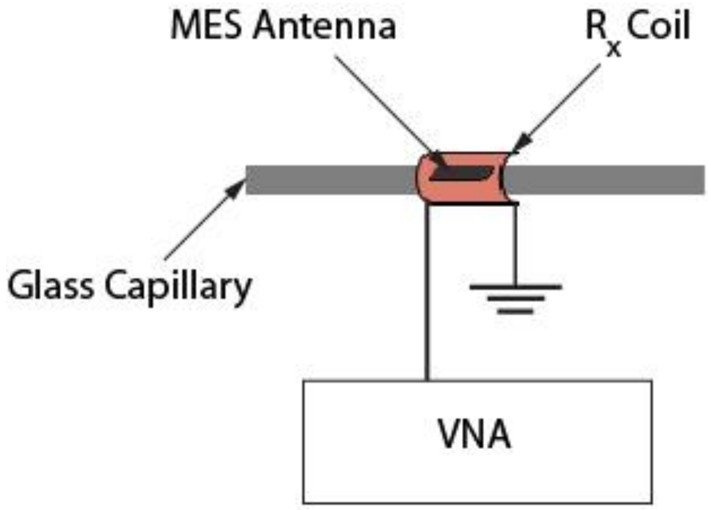

Figure 3. 1 Schematic diagram showing setup for wireless detection of MES antennas using a VNA

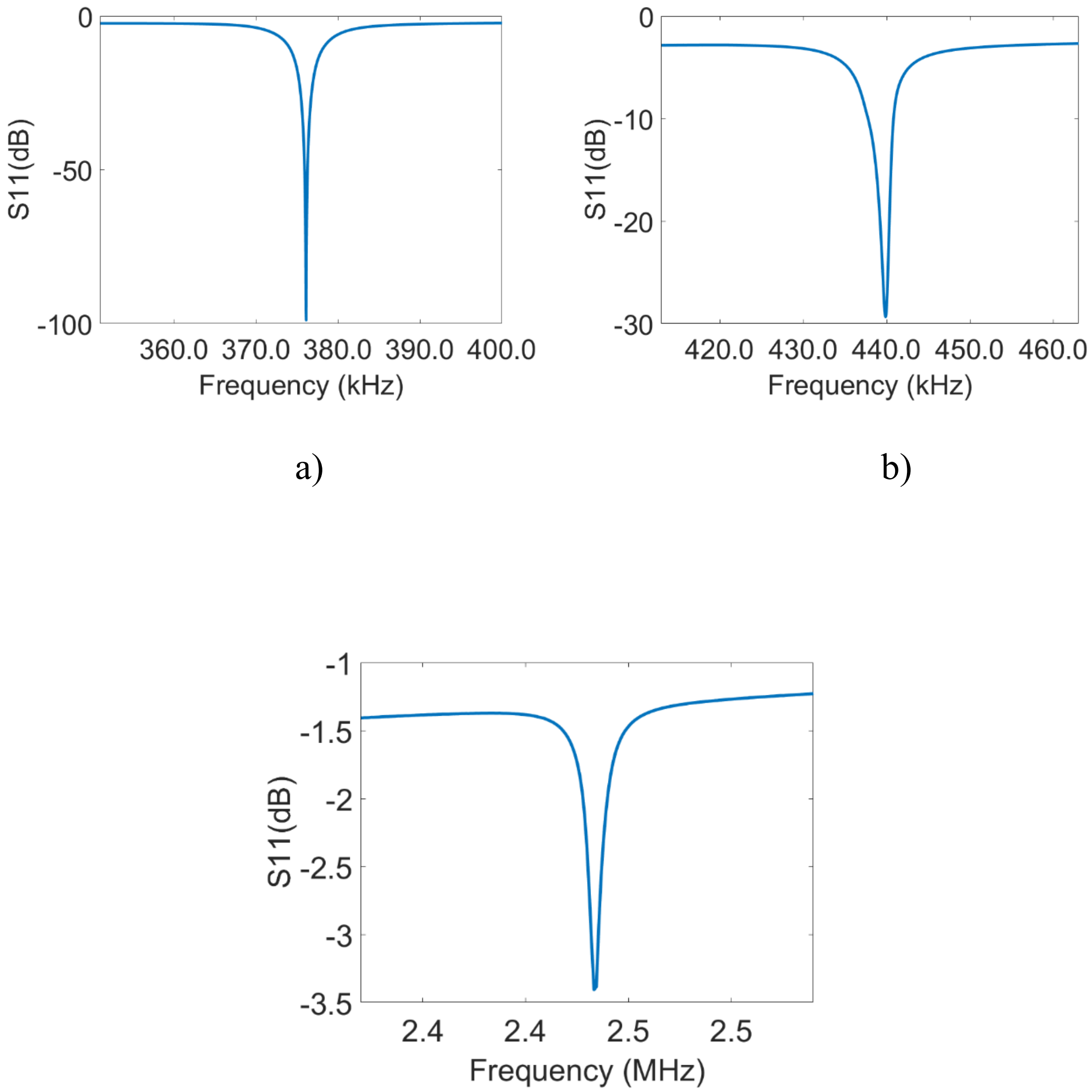

a) b)

c)

Figure 3. 2 Measured S11 vs Frequency plots for MES antennas of dimensions a) 6 mm x 1 mm x 28 um, b) 5 mm x 1 mm x 28 um, c) 1 mm x 500 um x 28 um

3.2.2 Lock-in Amplifier

Fig 3.3a shows a schematic diagram of the setup for wireless detection of MES antennas using a Lock-in Amplifier. It consists of two coils, one for excitation and the other for receiving the signal from the antenna. The transmission (Tx) coil is used to excite the resonator with a uniform AC magnetic field. The Receiving (Rx) coil is a gradiometer coil consisting of two identical coils connected in series and wound in opposite directions positioned inside the Tx coil such that the voltage induced on each solenoid is equal and opposite and the net voltage across it is zero when the resonator is not present inside. The MES antenna to be measured is placed inside one of the solenoids of the Rx coil during measurement. The Rx coil was designed to minimize the parasitic capacitance and maximize the self-resonance frequency (SRF). The SRF of the coil should be much greater than the frequency of interest since the antenna is inductively coupled to the coil. For a 500 um x 200 um x 28 um resonator having a resonance frequency of about 4.5 MHz an Rx coil having two solenoids of 2 mm diameter, 1 mm length and 26 turns made of a single layer of 47 AWG wire, with an SRF of over 100 MHz was used. A larger solenoid of 6 mm diameter 20 mm length and 40 turns made of 26 AWG wire was used as the Tx coil to provide a uniform AC magnetic field excitation of 6 Oe along the length of the resonator. The Tx coil is connected to the output of the lock-in amplifier and the Rx coil is connected to the input and the amplitude and phase of the voltage across the Rx coil as a function of frequency of the excitation magnetic field was measured. A permanent magnet was used to provide the optimum DC bias magnetic field. The detected voltage has a peak at the resonance frequency due to increase in the effective permeability at resonance. Fig 3.3b shows the coil voltage amplitude as a function of frequency measured in air using a lock-in amplifier for three different sub-mm resonators of dimensions 525 um x 200 um x 28um, 500 um x 200 um x 28 um and 400 um x 200 um x 28 um.

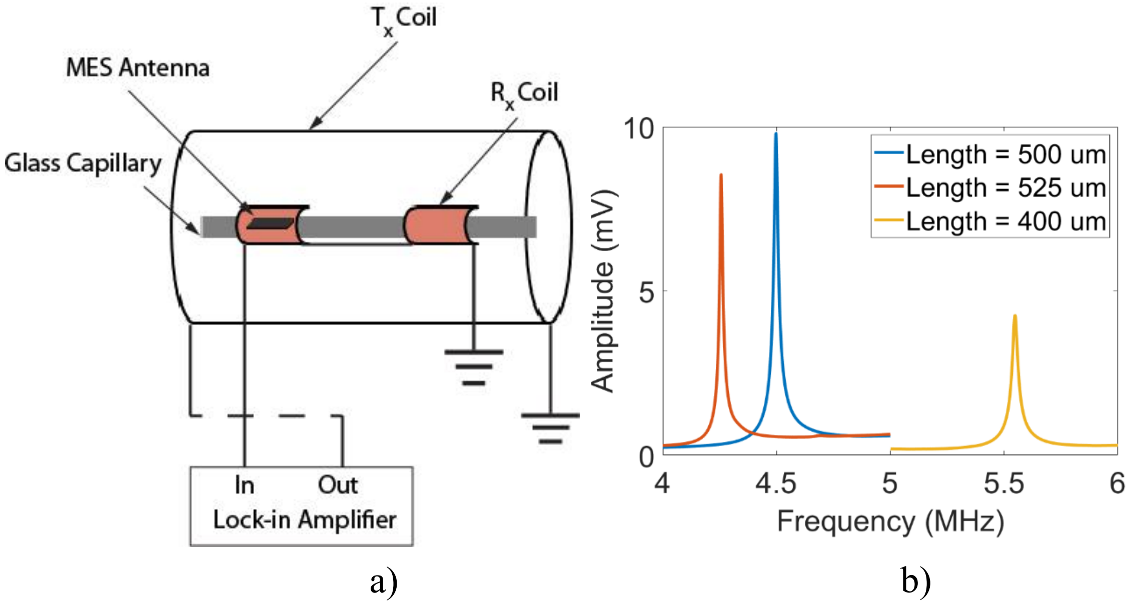

Figure 3. 3 a) Schematic diagram showing the setup for wireless detection of MES Antennas using a Lock-in-Amplifier. b) Measured coil voltage amplitude vs Frequency for sub-mm MES antennas

3.3 Modelling the Frequency Response of MES Antennas in Air

The frequency response of MES antennas in air is modelled using Finite Element Analysis and using analytical equations to estimate important parameters such as magnetostrictivity (d), Young's Modulus (E), magnetomechanical coupling coefficient (k^2) and Rayleigh damping coefficient (α). At the optimum DC bias, the behavior of a magnetostrictive material can be approximated using linear piezomagnetic governing equations as given below:

$$\boldsymbol{\varepsilon} = \boldsymbol{s_H S} + \boldsymbol{d_{HT}}^{\boldsymbol{T}} \boldsymbol{H} \tag{3.2}$$

$$\boldsymbol{B} = \boldsymbol{d_{HT} S} + \boldsymbol{\mu_0 \mu_r H} \tag{3.3}$$

where $\boldsymbol{\varepsilon}$, $\boldsymbol{S}$, $\boldsymbol{H}$, and $\boldsymbol{B}$ denote the strain, stress, magnetic field and magnetic flux density, $\boldsymbol{\mu_0}$ is the magnetic permeability of free space, $\boldsymbol{\mu_r}$ is the relative permeability at constant strain, and $\boldsymbol{s_H}$, $\boldsymbol{d_{HT}}$ denote the compliance matrix and piezomagnetic coupling matrix which is as given below for an isotropic magnetostrictive material:

$$\boldsymbol{d_{HT}} = \begin{bmatrix} \boldsymbol{d} & \mathbf{0} & \mathbf{0} & \mathbf{0} & \mathbf{0} & \mathbf{0} \\ \mathbf{0} & \boldsymbol{d} & \mathbf{0} & \mathbf{0} & \mathbf{0} & \mathbf{0} \\ \mathbf{0} & \mathbf{0} & \boldsymbol{d} & \mathbf{0} & \mathbf{0} & \mathbf{0} \end{bmatrix} \tag{3.4}$$

$$
\boldsymbol{s_H} = \begin{bmatrix} \mathbf{1/E} & \boldsymbol{-\nu/E} & \boldsymbol{-\nu/E} & \mathbf{0} & \mathbf{0} & \mathbf{0} \\ \boldsymbol{-\nu/E} & \mathbf{1/E} & \boldsymbol{-\nu/E} & \mathbf{0} & \mathbf{0} & \mathbf{0} \\ \boldsymbol{-\nu/E} & \boldsymbol{-\nu/E} & \mathbf{1/E} & \mathbf{0} & \mathbf{0} & \mathbf{0} \\ \mathbf{0} & \mathbf{0} & \mathbf{0} & \boldsymbol{(1+\nu)/E} & \mathbf{0} & \mathbf{0} \\ \mathbf{0} & \mathbf{0} & \mathbf{0} & \mathbf{0} & \boldsymbol{(1+\nu)/E} & \mathbf{0} \\ \mathbf{0} & \mathbf{0} & \mathbf{0} & \mathbf{0} & \mathbf{0} & \boldsymbol{(1+\nu)/E} \end{bmatrix} \tag{3.5}
$$

where d is the magnetostrictivity at optimum DC bias, E the Young's modulus and ν the poisson's ratio of the material. A Rayleigh damping factor (α) is introduced to account for structural damping effects. Based on the above governing equations and the equations of motion we can model the frequency response of MES antennas when excited by an AC magnetic field of certain frequency. The modelling is done using Finite Element Analysis Software Comsol Multiphysics as well as using analytical equations in Matlab. The magnetostrictivity and Young's Modulus of the material depend on the fabrication conditions and their values have been estimated to best fit the experimental data with the simulation. The material properties used for Metglas 2826 MB are as shown in Table 2.1. An MES antenna of dimensions 475 um x 200 um x 28 um is considered for all simulations discussed in this section.

Table 3. 1 Material properties of Metglas 2826 MB

Material property	Value
Density (kg/m^3)	7900
Young's Modulus (GPa)	160.0
Magnetostrictivity (m/A)	0.97 x $\mathbf{10^{-9}}$
Poisson's Ratio	0.22
AC Relative Permeability (4.5 MHz)	20.0

3.3.1 Comsol Simulation

Finite Element Analysis (FEA) is a universal tool for modelling the frequency response of a magnetoelastic resonator since it can be applied to model any resonator geometry and any coil configuration. The Magnetostriction module in Comsol Multiphysics which couples the AC/DC module and Structural Mechanics module is used for the simulation. A 3D domain is used for the simulation since the problem lacks any 2D symmetry. The resonator is modelled as a 475 um x 200 um x 28 um domain having the material properties as listed in Table 3.1. The mid-plane of the resonator is assigned as a fixed boundary since it is a nodal plane and all other surfaces are assigned as free. A large air domain is created around the resonator to model the magnetic flux density using Ampere's law. A magnetic insulation boundary condition is applied for the air boundaries to prevent any flux leakage. A homogenized current-carrying domain with 26 turns of 47 AWG wire around the resonator is used to model the Rx coil. A uniform AC magnetic field of 6 Oe, equal to the experimentally applied magnetic field is used for exciting the magnetostrictive material along its length and the frequency of the field is swept to model the frequency response of the resonator. Fig. 3.4a shows the simulated tip displacement of the resonator as a function of frequency of excitation magnetic field. The resonance frequency in air is shown to be 4.67 MHz where the tip displacement is maximum. Fig. 3.4b and Fig. 3.4c shows the distribution of strain and magnetization in the resonator at the resonance frequency respectively, which are identical since magnetization in the material is a function of the strain as given by equation 3.3. Fig 3.5a and Fig 3.5b shows the distribution of magnetic flux density in the central plane of the coil without and with the resonator inside at the resonance frequency. It can be observed that the magnetic flux density in Fig 3.5b is much higher due to the high effective permeability of the magnetostrictive material which in turn is a function of strain in the material as observed from Fig 3.4 b and c. Fig 3.6 shows the simulated and experimental coil voltage and amplitude which can been seen to be in good agreement. The resonator is found to have a high mechanical quality factor of 510.0 and magnetomechanical coupling coefficient (k^2) of 1.10%.

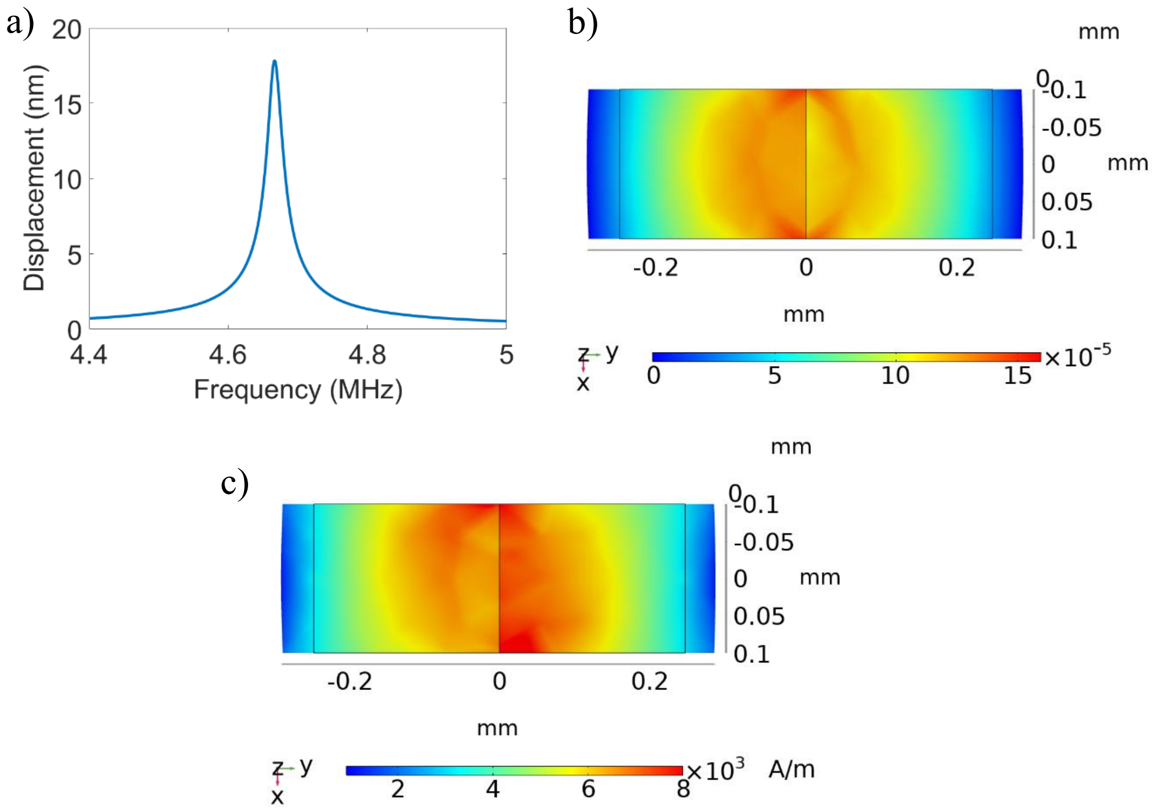

Figure 3. 4 Simulation results for a 475 um x 200 um x 28 um MES Antenna. a) Tip displacement vs Frequency of excitation. b) Distribution of strain in the resonator at resonance frequency (4.67 MHz). c) Distribution of magnetization in the resonator at the resonance frequency (4.67 MHz)

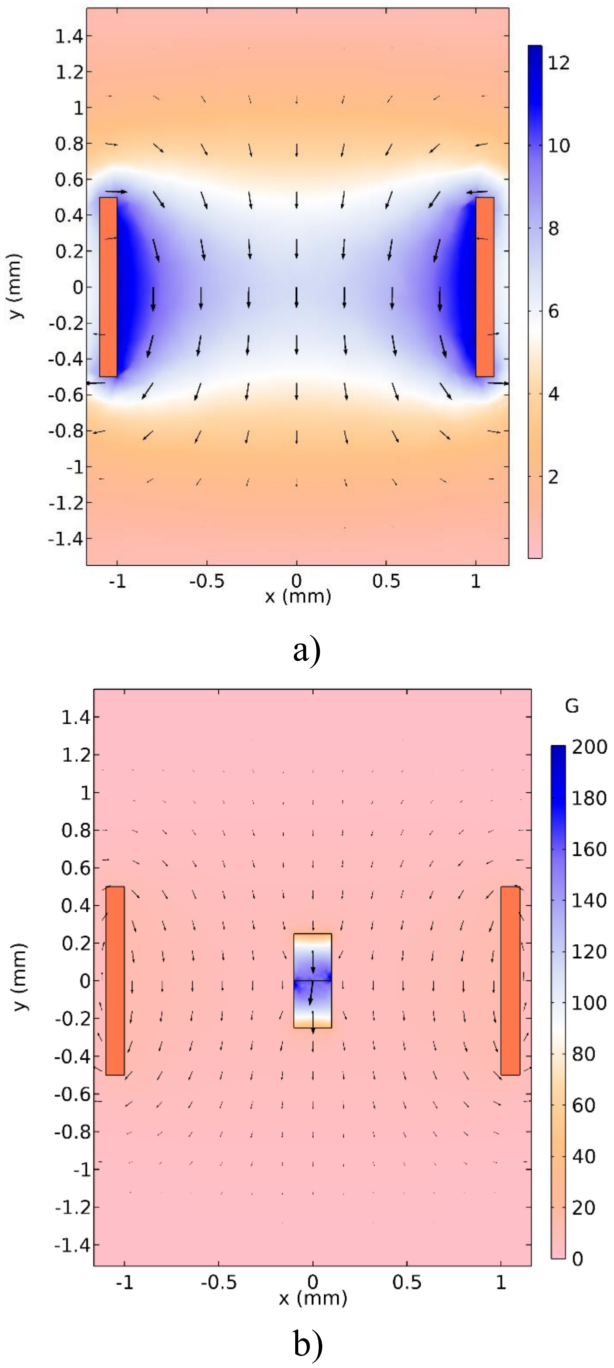

Figure 3. 5 Magnetic field distribution inside the Rx coil a) without and b) with the resonator of 475 um x 200 um x28 um inside at the resonance frequency (4.67 MHz)

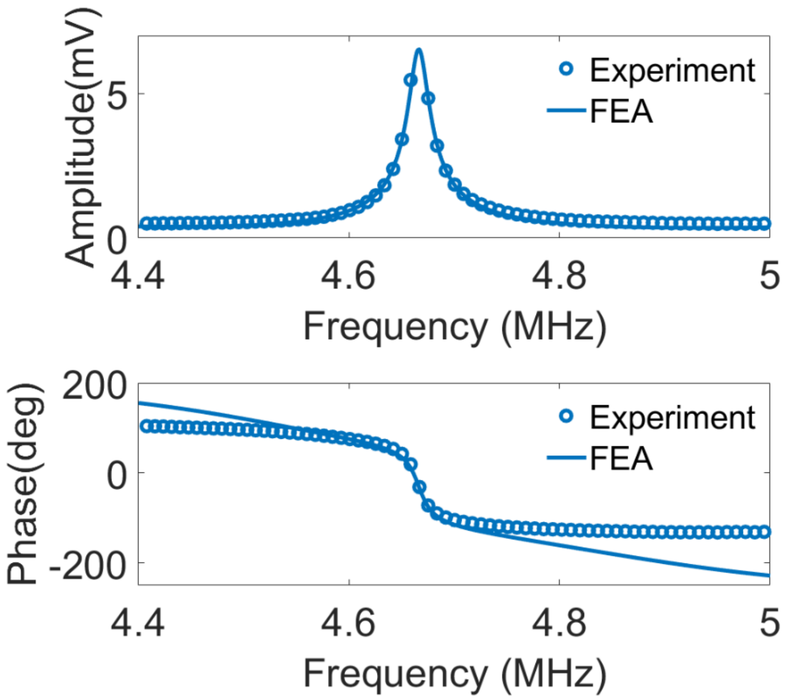

Figure 3. 6 Comparison of coil voltage amplitude and phase obtained from experiment and FEA simulation

3.3.2 Analytical Modelling

The frequency response of MES antennas was also modelled using one-dimensional analytical equations [10]. We consider an MES antenna of length $\boldsymbol{2L}$, width $\boldsymbol{w}$ and thickness $\boldsymbol{t_s}$, with length along the x-axis and centred at the origin. The 3D constitutive equations as described by equation (3.2) and equation (3.3) is reduced into 1D equations by assuming that the stresses and strains are confined to the longitudinal direction of the resonator. Equations (3.2) and (3.3) can be simplified to obtain:

$$\boldsymbol{\varepsilon_{xx} = \frac{\sigma_{xx}}{E} + dH_x} \tag{3.6}$$

$$\boldsymbol{B_x = d\sigma_{xx} + \mu_0\mu_r H_x} \tag{3.7}$$

where $\boldsymbol{\varepsilon_{xx}}$, $\boldsymbol{\sigma_{xx}}$, $\boldsymbol{H_x}$, $\boldsymbol{B_x}$, and $\boldsymbol{H_x}$ denote the normal strain, normal stress, magnetic field and magnetic flux density in the x-direction. Equations (5) and (6) can be rearranged in terms of $\boldsymbol{\sigma_{xx}}$ and $\boldsymbol{H_x}$ as:

$$\boldsymbol{\sigma_{xx} = E_{app}\varepsilon_{xx} - \frac{E_{app}d'}{\mu_0{\mu_r}'}B_x} \tag{3.8}$$

$$\boldsymbol{H_x = -\frac{E_{app}d'}{\mu_0{\mu_r}'}\varepsilon_{xx} + \frac{1}{\mu_0{\mu_r}'}B_x} \tag{3.9}$$

where,

$$\boldsymbol{E_{app} = \frac{E\mu_0\mu_r}{\mu_0\mu_r - d^2E}} \tag{3.10}$$

$$\boldsymbol{\mu_0\mu_r' = \mu_0\mu_r - d^2E} \tag{3.11}$$

$$\boldsymbol{d' = \frac{d(\mu_0\mu_r - d^2E)}{\mu_0\mu_r}} \tag{3.12}$$

The governing equation is derived by applying Newton's second law to an infinitesimal section of the resonator as shown in Fig. 3.7. The displacement of the infinitesimal mass is denoted by the function $\boldsymbol{u(x,t)}$, where:

$$\boldsymbol{\varepsilon_{xx}} = \frac{\partial \boldsymbol{u}}{\partial \boldsymbol{x}} \tag{3.13}$$

The structural damping force $\boldsymbol{F_{struc}}$ shown in Fig. 3.7 is modelled by considering Rayleigh damping with a damping parameter ($\boldsymbol{\alpha}$). For a resonator of mass m, density ρ and cross-sectional area A, $\boldsymbol{F_{struc}}$ can be written as:

$$\boldsymbol{F_{struc}} = \boldsymbol{\alpha m} = \boldsymbol{\alpha \rho A} \tag{3.14}$$

The simplified governing equations for the vibration of the resonator are as given below:

$$\left(\boldsymbol{E_{app}} - \frac{\boldsymbol{d'^2 E_{app}}^2}{\boldsymbol{\mu_0 \mu_r'}}\right) \boldsymbol{t_s} \frac{\partial^2 \boldsymbol{u}}{\partial \boldsymbol{x}^2} - \boldsymbol{\rho t_s} \frac{\partial^2 \boldsymbol{u}}{\partial \boldsymbol{t}^2} - \boldsymbol{\alpha \rho t_s} \frac{\partial \boldsymbol{u}}{\partial \boldsymbol{t}} = \boldsymbol{E_{app} d t_s} \frac{\partial \boldsymbol{H_x}}{\partial \boldsymbol{x}} \tag{3.15}$$

which can be solved using eigenfunction expansion to obtain the solution for $u(x,t)$ as described in Ref. [10]. The voltage and phase of the coil wrapped around the resonator is given by the rate of change of magnetic flux density inside the coil. The resonator is assumed to be a magnetic dipole of length $2L$ to estimate the magnetic flux density distribution in the air around the resonator. Values for different material parameters are same as that given in Table 3.1. Fig. 3.6 shows the comparison between coil voltage amplitude and phase for the experiment and Analytical model for a 475 um x 200 um x 28 um resonator which can be seen to be in good agreement.

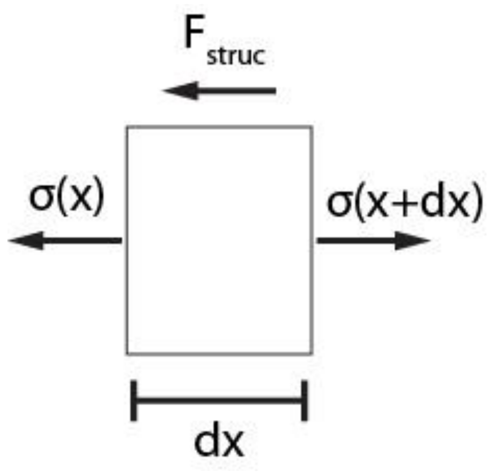

Figure 3. 7 Free body diagram showing an infinitesimal section of the magnetoelastic resonator and the forces acting on it.

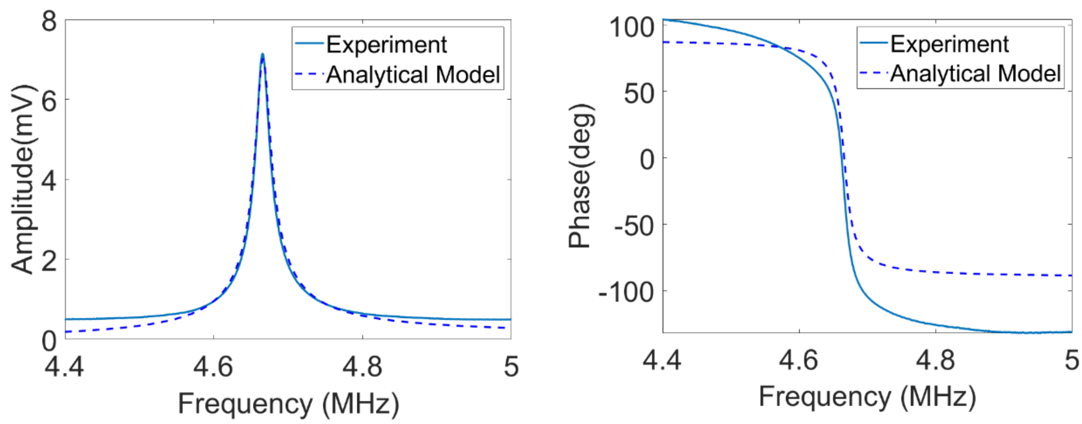

Figure 3. 8 Comparison of coil voltage amplitude and phase obtained from experiment and Analytical model

3.4 Measurement in Water

The MES antennas are next characterized in water to understand the frequency response in a wet environment. The setup in Fig 3.3a is modified by filling the capillary tube containing the resonator with water during the measurement. Fig. 3.9 shows a comparison between detected coil voltage and phase in air and water as a function of frequency of excitation magnetic field. Viscous damping reduces the quality factor from 510.0 in air to 68.0 in water and the resonance frequency shifts from 4.67 MHz in air to 4.60 MHz in water due to mass loading effects. Hence, the resonators can still function in a wet environment even though the quality factor is reduced. This reduces the signal to noise ratio and frequency stability of the resonator which adversely affects the sensitivity in water compared to air which is discussed in the next chapter. Despite the reduction in sensitivity, it will be shown that miniature MES antennas can find useful applications for wireless sensing of analytes such as pH in biological fluids.

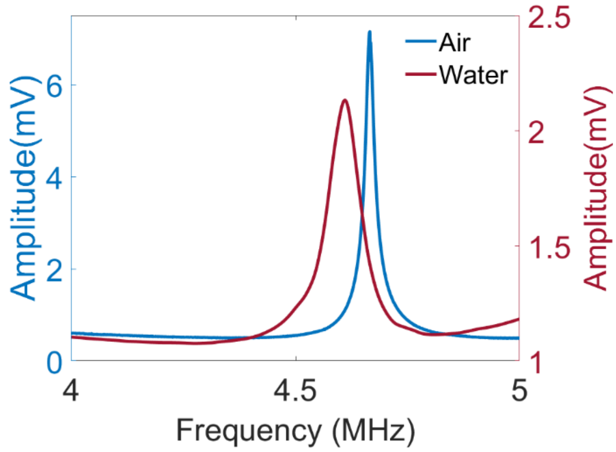

a)

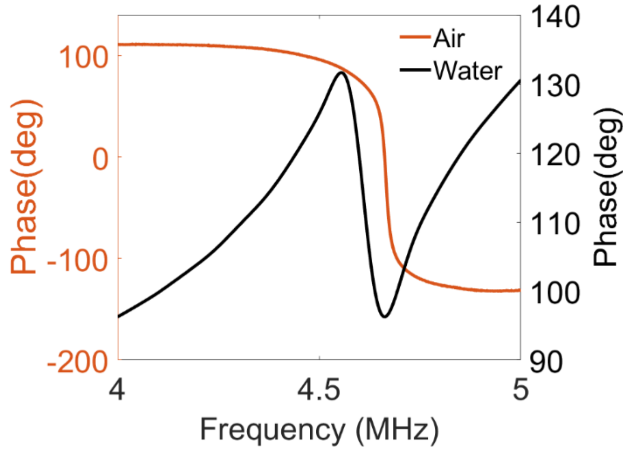

b)

Figure 3. 9 Comparison of coil voltage a) amplitude and b) phase for 475 um x 200 um x 28 um MES antenna measured in air and water

Chapter 4

pH Sensing Using MES Antennas

4.1 Introductory remarks

MES antennas have been shown to be useful for sensing gases such as ammonia, liquid viscosity, bacterial concentration etc. [1]. Here a miniature MES antenna of dimensions 6 mm x 1 mm x 28 um which can be used for sensing pH wirelessly is discussed. MES antennas can operate as sensors because their resonance frequency depends on the mass of the resonator and hence if the mass of the resonator changes in response to a change in the concentration of an analyte of interest there is a shift in the resonance frequency. This can be achieved by chemically functionalizing the resonators with molecules which can bind to an analyte or swell/shrink in response to a change in concentration of the analyte. The shift in resonance frequency of the resonator is given by the formula:

$$\Delta \boldsymbol{f} = -\frac{\boldsymbol{f}}{\mathbf{2}}\frac{\Delta \boldsymbol{m}}{\boldsymbol{M}} \tag{4.1}$$

where Δm is the change in mass, M is the original mass and f the original resonance frequency. Since the sensitivity, $\frac{\Delta f}{\Delta m} = -f/2M$, it increases as the antenna size is scaled down. Magnetoelastic sensors for pH sensing have been reported earlier. Here a miniaturized MES antenna of higher sensitivity for pH sensing is shown, which can achieve a 5 times higher sensitivity compared to previously reported studies ([11]–[13]). A pH sensitive hydrogel made of Acrylic Acid and Isooctyl Acrylate is used to functionalize the MES antennas, which swell/shrink in response to pH change causing a shift in the resonance frequency [14].

4.2 pH Sensitive Polymer Synthesis

The polymer chosen for functionalization is Polyacrylic Acid hydrophobically modified with 20% Isooctyl Acrylate (IOA). The copolymer is synthesized by free radical copolymerization of 5 mL of Acrylic Acid (AA) with 3.95 mL of IOA in 25 mL DMF in a 100 mL round bottom flask. 70 mg (0.5 mol %) of initiator 2,2'-azobisisobutyronitrile (AIBN) and 70 mg (0.5 mol%) of cross-linker *N*,*N*-methylenebisacrylaminde (MBAA) was added to the mixture after it was bubbled with nitrogen for 30 min. The mixture was then transferred to an oil bath at 65°C and the reaction was allowed to proceed for 6 hours. The synthesized polymer solution was recrystallized by dissolving in ethanol and precipitating into large volume of Diethyl

Ether. The purified polymer is dried in a vacuum oven at 1 Torr pressure at 100°C. The dried polymer is soluble in ethanol but not soluble in water.

4.3 Functionalization of MES Antennas with pH Sensitive Polymer

The polymer has to be chemically functionalized to the resonator surface for pH sensing, since swelling produces a lot of stress which causes the films to delaminate if it is loosely bound to the surface. Polyurethane was used as an adhesive layer for the functionalization. 6 mm x 1 mm x 28 um resonators were first coated with a 3 um layer of Polyurethane by dip coating the resonator in a 40% solution of Polyurethane in water. The sensors were dried in air for 10 min and then dried at 150 °C for 2 hours in a vacuum oven at 10 Torr pressure. Next the resonators were incubated for 2 hours at room temperature in a 0.075 g/mL solution of the pH sensitive hydrogel in ethanol with 10 mg/mL EDC (1-Ethyl-3-(3-dimethylaminopropyl)carbodiimide) and 10 mg/mL NHS (*N*-Hydroxysuccinimide). EDC/NHS reaction helps in chemically binding the amine groups in polyurethane to carboxylic acid groups in Polyacrylic acid by forming amide bonds. Dip coating can be used to adjust the thickness of the polymer layer formed. Different polymer thicknesses are used to study the sensitivity of the pH sensor. After incubation the resonators are dried in a vacuum oven for 2 hours at 1 Torr pressure at 100 °C. The dried resonators are used for sensing experiments. First the sensor surface is observed using a microscope to observe the swelling behavior of the polymer. Fig 4.1a and Fig 4.1b shows the resonator surface in acidic (pH=4.0) and basic (pH=8.6) pH respectively. It can be seen that the polymer on the sensor surface swells in basic medium. The swelling can be explained by the difference in osmotic pressure between the gel and the surrounding solution which is caused due to the ionization of the fixed carboxylic acid molecules in the polymer matrix. In the next section the frequency response of the resonators in solutions of different pH is studied to characterize their sensitivity and repeatability.

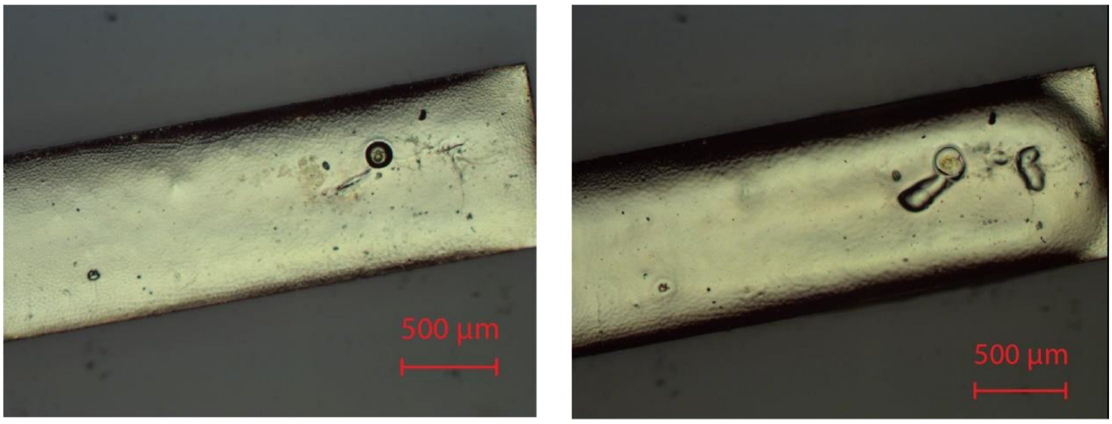

a) b)

Figure 4. 1 Optical images of a 6 mm x 1 mm x 28 um resonator coated with pH sensitive polymer in a) Acidic (pH=4.0) and b) basic (pH=8.6) solution

4.4 pH Sensing Using MES Antennas

The same setup shown in Fig 3.1 is used for the pH sensing experiments. Solutions of different pH ranging from 4.4 to 8.6 were prepared 0.05 M Acetic Acid and 0.05 M $\mathbf{K_2HPO_4}$. The pH values were adjusted using 1 M HCl or 1 M NaOH and calibrated using a pH meter. The solutions of different pH are flowed into the capillary tube containing the resonator and the resonance frequency is recorded. Fig 4.2a shows the recorded resonator response for 6 mm x 1mm x 28 um coated with a 5 um thick layer of the pH sensitive polymer for different pH solution ranging from 4.4 to 6.2. The resonator shows a sensitivity of 15 kHz/pH and can detect pH changes of 0.01 in the above range. The resonator is too damped for solutions having pH greater than 6.2. Hence a thinner polymer coating was used to achieve sensing for a larger pH range. Fig 4.2b shows the resonator response for a 6 mm x 1 mm x 28 um sensor coated with 1 um thick layer of pH sensitive polymer. A wide range of pH from 4.76 to 8.36 can be sensed using 1 um thick coating of the polymer although the sensitivity is reduced to 3.5 kHz/pH. Fig 4.4 also shows reversible sensing by cycling between different pH values and it can be seen that the response is reversible and repeatable.

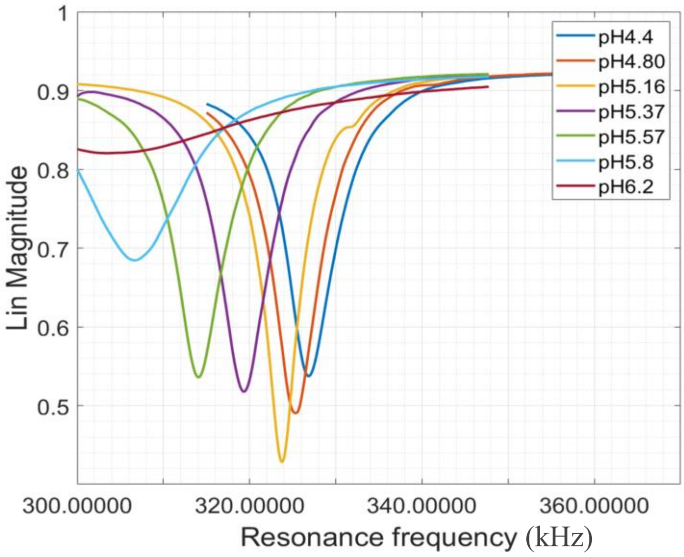

a)

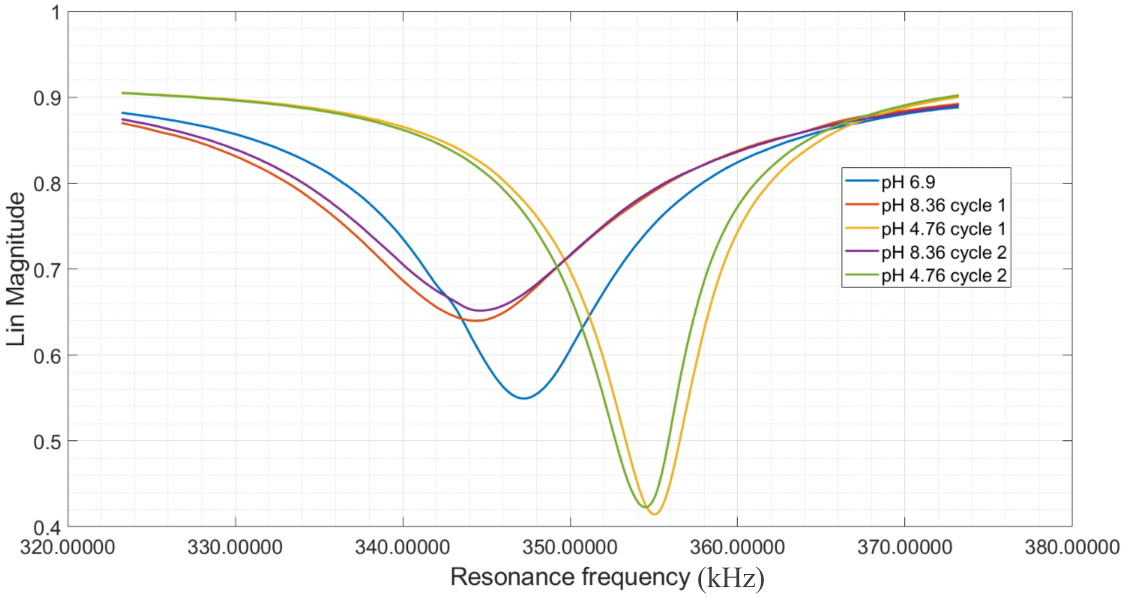

b)

Figure 4. 2 S11 vs frequency of a 6 mm x 1 mm x 28 um resonator coated with a) 5 µm and b) 1 µm thick layer of pH sensitive polymer in different pH solutions

4.5 Discussion

A miniature MES antenna for wirelessly sensing pH in fluids was demonstrated with a higher sensitivity than previously reported studies. Future work involves characterization of the antennas in biological fluids and detection from outside the solenoid coil to explore in-vivo applications of the sensors. Also, sensing using sub-mm antennas should be explored to increase sensitivity and widen the applications possible. Preliminary experiments with sub-mm antennas were unsuccessful due to delamination of pH sensitive polymer during swelling. Further study on the chemical functionalization and swelling dynamics is needed to enable sub-mm MES antennas for pH sensing.

Chapter 5

Conclusion and Future Work

5.1 Conclusion

In this thesis I have explored fabrication of miniaturized MES antennas using Diesaw and Laser Micromachining. MES antennas of sizes as small as 400 um x 200 um x 28 um was fabricated using Laser Micromachining and Diesaw. It was found that Laser Micromachining is a more versatile fabrication method compared to fabrication using a Diesaw since it can be used to fabricate any antenna shape and doesn't involve time consuming sample preparation and post processing steps. The smallest antennas fabricated were found to have a high mechanical Q-factor of 510.0 in air and 68.0 in water with a magnetimechnical coupling coefficient of 1.10 % and were found to be suitable for wireless sensing applications in liquid media. The modelling using Finite Element analysis and analytical equations were found to match well with the experiment and can be used for designing coils for future in-vivo applications. A pH responsive hydrogel was synthesized and the MES antennas were functionalized with polymer of different thicknesses to fabricate sensors with different sensitivities. A high sensitivity of 15 kHz/pH was observed for a polymer coating of 5 um with a range of sensitivity from pH 4.4 to pH 6.2 for a 6 mm x 1 mm x 28 um MES antenna in liquid medium.

5.2 Future Work

Laser micromachining has been shown to enable fabrication of MEMS structures as small as 20 um [9]. Future work involves optimization of laser parameters for fabrication of smaller resonators. For sub-mm antennas, annealing in transverse magnetic field has to be explored to improve the signal level and enable detection outside the coil for future in-vivo applications. Fabrication of more sensitive pH sensors have to be explored by carefully studying the swelling dynamics and stresses involved during pH responsive swelling of the synthesized hydrogel. Other chemical functionalization to fabricate MES antennas which can sense different analytes is also worth exploring.

Bibliography

[1] L. Ren, K. Yu, and Y. Tan, "Applications and Advances of Magnetoelastic Sensors in Biomedical Engineering: A Review," *Materials*, vol. 12, no. 7, 2019, doi: 10.3390/MA12071135.

[2] C. Rowell and E. Y. Lam, "Mobile-phone antenna design," *IEEE Antennas and Propagation Magazine*, vol. 54, no. 4, pp. 14–34, 2012, doi: 10.1109/MAP.2012.6309152.

[3] J. Thimot and K. L. Shepard, "Bioelectronic Devices: Wirelessly powered implants," 2017, doi: 10.1038/s41551-017-0051.

[4] "IEEE C95.1-2019 - IEEE Standard for Safety Levels with Respect to Human Exposure to Electric, Magnetic, and Electromagnetic Fields, 0 Hz to 300 GHz." https://standards.ieee.org/standard/C95_1-2019.html (accessed Jul. 23, 2021).

[5] B. A. Kramer, C. C. Chen, M. Lee, and J. L. Volakis, "Fundamental limits and design guidelines for miniaturizing ultra-wideband antennas," *IEEE Antennas and Propagation Magazine*, vol. 51, no. 4, pp. 57–69, Aug. 2009, doi: 10.1109/MAP.2009.5338684.

[6] A. K. Skrivervik, J. F. Zürcher, O. Staub, and J. R. Mosig, “PCS antenna design: The challenge of miniaturization,” *IEEE Antennas and Propagation Magazine*, vol. 43, no. 4, pp. 12–27, Aug. 2001, doi: 10.1109/74.951556.

[7] J. P. Domann and G. P. Carman, “Strain powered antennas,” *Journal of Applied Physics*, vol. 121, no. 4, p. 044905, Jan. 2017, doi: 10.1063/1.4975030.

[8] Y. Liu *et al.*, “Highly sensitive surface-scanning detector for the direct bacterial detection using magnetoelastic (ME) biosensors,” *SPIE*, vol. 10217, p. 1021703, May 2017, doi: 10.1117/12.2262859.

[9] “Laser Direct-Write Fabrication of MEMS by Prashant Patil,” 2011.

[10] S. R. Green and Y. B. Gianchandani, “Wireless magnetoelastic monitoring of biliary stents,” *Journal of Microelectromechanical Systems*, vol. 18, no. 1, pp. 64–78, 2009, doi: 10.1109/JMEMS.2008.2008568.

[11] C. Ruan, K. Zeng, and C. A. Grimes, “A mass-sensitive pH sensor based on a stimuli-responsive polymer,” *Analytica Chimica Acta*, vol. 497, no. 1–2, pp. 123–131, Nov. 2003, doi: 10.1016/J.ACA.2003.08.051.

[12] C. Schanzenbach *et al.*, “Preparation and characterisation of a sensing system for wireless pH measurements in vivo, in a rumen of a cow,” *Sensors and Actuators B: Chemical*, vol. 242, pp. 637–644, Apr. 2017, doi: 10.1016/J.SNB.2016.11.089.

[13] C. QY and G. CA, “A remote query magnetoelastic pH sensor,” *Sensors and actuators. B, Chemical*, vol. 71, no. 1–2, pp. 112–117, Nov. 2000, doi: 10.1016/S0925-4005(00)00599-2.

[14] Olga E. Philippova, Dominique Hourdet, and Roland Audebert, and A. R. Khokhlov†, “pH-Responsive Gels of Hydrophobically Modified Poly(acrylic acid),” *Macromolecules*, vol. 30, no. 26, pp. 8278–8285, Dec. 1997, doi: 10.1021/MA970957V.